THE JOURNAL OF BIOLOGICAL CHEMISTRY Vol. 274, No. 42, Issue of October 15, pp. 29937–29943, 1999
Printed in U.S.A.

Interaction of Macrophage-stimulating Protein with Its Receptor

RESIDUES CRITICAL FOR β CHAIN BINDING AND EVIDENCE FOR INDEPENDENT α CHAIN BINDING*

(Received for publication, May 13, 1999, and in revised form, July 7, 1999)

Alla Danilkovitch‡§, Maria Miller¶, and Edward J. Leonard‡

From the ‡Laboratory of Immunobiology, NCI-Frederick Cancer Research and Development Center and ¶Macromolecular Structure Laboratory, NCI-Frederick Cancer Research and Development Center, ABL-Basic Research Program, Frederick, Maryland 21702

Macrophage-stimulating protein (MSP) and hepatocyte growth factor/scatter factor (HGF/SF) are plasminogen-related growth and motility factors that interact with cell-surface protein tyrosine kinase receptors. Each one is a heterodimeric protein comprising a disulfide-linked α chain and a serine protease-like β chain. Despite structural similarities between MSP and HGF, the primary receptor binding site is located on the α chain of HGF/SF but on the β chain of MSP. To obtain insight into the structural basis for MSP β chain binding, β chain structure was modeled from coordinates of an existing model of the HGF β chain. The model revealed that the region corresponding to the S1 specificity pocket in trypsin is filled by the Asn^{682}/Glu^{648} interacting pair, leaving a shallow cavity for possible β chain interaction with the receptor. Mutants in this region were created, and their binding characteristics were determined. A double mutation of Asn^{682}/Glu^{648} caused diminished binding of the β chain to the MSP receptor, and a single mutation of neighboring Arg^{683} completely abolished binding. Thus, this region of the molecule is critical for binding. We also found that at equimolar concentrations of free α and β chains, α chain binding to receptor was detectable, at levels considerably lower than β chain binding. The EC_{50} values determined by quantitative enzyme-linked immunosorbent assay are 0.25 and 16.9 nM for β and α chain, respectively. The data suggest that MSP has two independent binding sites with high and low affinities located in β and α chain, respectively, and that the two sites together mediate receptor dimerization and subsequent activation.

Macrophage-stimulating protein (MSP)[1] is a 78-kDa growth and motility factor that belongs to a plasminogen-related kringle protein family (1, 2). It is most closely related to hepatocyte growth factor/scatter factor (HGF/SF), to which it has 45% sequence similarity (3). Mature MSP acts on a number of cell types including tissue macrophages, epithelia, and hematopoietic cells (4). Actions on macrophages include stimulation of motility (5), induction of phagocytosis of serum complement-coated erythrocytes (1), inhibition of inducible NO synthase up-regulation by inflammatory stimuli (6), and induction of interleukin 6 secretion.[2] MSP induces adhesion, motility, and replication of epithelial cells, and it can prevent the apoptosis that occurs when epithelial cells are prevented from attachment to a substrate (7). MSP mediates its effects by binding to and activating a cell receptor tyrosine kinase known as RON in humans (8, 9) and STK in mice (10, 11). Closely related HGF/SF also has mitogenic and motogenic actions on epithelial cell types (12) that express Met, the specific receptor for this ligand (13). HGF has a morphogenetic role in development and tissue repair (14). Specific mutations in Met are oncogenic in both experimental models (for a review see Ref. 15) and in sporadic human cancers (16).

In contrast to other members of this plasminogen-related family, which are serine proteases, MSP and HGF are devoid of enzymatic activity because of catalytic triad mutations. However, they have retained the proteolytic mechanism of activation of the zymogens of the family (17). Thus, MSP is synthesized by hepatocytes (18) as biologically inactive single chain pro-MSP and is converted at extravascular sites to active MSP by trypsin-like proteases, which cleave at Arg^{483}/Val^{484} (19) to make a disulfide-linked αβ chain heterodimer (20). MSP and HGF have 40% sequence similarity to plasminogen and the same domain organization. The three proteins evolved from a common ancestor (21). Features of the α chain of MSP and HGF include an N-terminal domain (N domain) corresponding to the plasminogen preactivation peptide, four kringles, and a segment that terminates in the cleavage site for activation; the β chain is the serine protease-like domain. HGF binds with high affinity to its receptor via the α chain. The N domain makes a critical contribution to HGF binding, since N domain deletion mutants have reduced or absent biological activity (22, 23) and fail to inhibit binding of HGF to Met-expressing target cells (23). In contrast to HGF, studies with ^{125}I-labeled subunits of MSP showed that the β chain bound with high affinity to RON, whereas α chain binding was undetectable (24). Mutant MSP lacking the β chain is biologically inactive (25). Therefore, despite the similarity in domains of HGF and MSP, the loci for high affinity binding to their receptors are completely different.

To explore the basis of MSP β chain binding to RON, we took advantage of a recently published energy-minimized three-dimensional model of the β chain of HGF (21). We used the HGF model coordinates to make a comparable model of the MSP β chain to look for features that might account for its binding properties. By analogy to proteases, MSP and HGF correspond to enzymes, and their receptors correspond to enzyme substrates. From this viewpoint, regions of the MSP serine protease-like domain of particular interest for binding to receptor would include the catalytic site and several surface

* This work was supported in part by funds from the National Cancer Institute, DHHS, under contract with ABL (to M. M.). The costs of publication of this article were defrayed in part by the payment of page charges. This article must therefore be hereby marked "*advertisement*" in accordance with 18 U.S.C. Section 1734 solely to indicate this fact.

§ To whom correspondence should be addressed: NCI-FCRDC, Bldg. 560/Rm. 12-46, Frederick, MD 21702. Tel.: 301-846-1560; Fax: 301-846-6145; E-mail:danilkovitch@mail.ncifcrf.gov.

[1] The abbreviations used are: MSP, macrophage-stimulating protein; HGF/SF, hepatocyte growth factor/scatter factor; MDCK, Madin-Darby canine kidney; CHO, Chinese hamster ovary; ELISA, enzyme-linked immunosorbent assay; PAGE, polyacrylamide gel electrophoresis.

[2] A. Skeel and E. J. Leonard, unpublished data.

loops that define the substrate binding cleft for chymotrypsin-like proteases (26). Our model of the MSP β chain revealed features that were postulated to account for its binding to RON. Mutagenesis studies reported herein established that the region corresponding to an enzyme S1 site is essential for β chain binding to RON.

Our experiments also revealed binding to RON-expressing cells of MSP-free α chain, which was a small fraction of the amount of β chain binding. This suggests that MSP has two receptor binding sites, a high affinity site in the β chain and a low affinity site in the α chain. The result supports a recent hypothesis that ligand-induced RON dimerization by MSP is mediated by a single ligand molecule, which binds to a receptor via the β chain, after which a second receptor is engaged by the α chain (27).

EXPERIMENTAL PROCEDURES

Materials—Human recombinant MSP and free α and β chains were from Toyobo (Osaka, Japan) and R & D Systems (Minneapolis, MN). Rabbit and mouse anti-MSP antibodies were described (28). Madin-Darby canine kidney (MDCK) and CHO-K1 cells were from ATCC (Manassas, VA). MDCK cells stably transfected with a human RON cDNA (clone RE7) were described (9).

Modeling of the MSP β Chain—Inasmuch as the MSP β chain has 48% amino acid identity to the HGF β chain, we used the coordinates of the three-dimensional model of the HGF β chain (21) to model the MSP β chain structure. Side chains of HGF were replaced with MSP side chains according to the alignment shown in Fig. 1. Positions of the conserved backbone atoms were not altered. The loop comprising residues 525–533 was modeled to reflect the experimentally demonstrated disulfide bridge between Cys^{527} and Cys^{562} (19). Subsequently the positions of several side chains were adjusted manually (program FRODO and its silicon graphics version TOM (29)) to remove bad contacts and to optimize electrostatic and hydrophobic interactions. The model was then energy-minimized using program XPLOR (30) employing 250 cycles of the Powell conjugate gradient algorithm.

Generation of Mutants of Wild Type Human MSP cDNA—All mutants were generated using the pAlterII (Promega, Madison, WI) mutagenesis kit with mutagenic oligonucleotides as follows: for R683Q, GGAATTATAATCCCCAACCAAGTATGCGCAAGGTCCCGC; for E648G/D682G, ATGTGCACTGGGGGACTGTTG/ATAATCCCCGGCCGAGTATGC. For stable transfection of eukaryotic cells wild type and mutant MSP were re-cloned into pCL-neo (Promega, Madison, WI).

Cell Culture and Transfection of Recombinant MSP—CHO-K1 cells (ATCC) were grown in Dulbecco's modified Eagle's medium supplemented with 8% fetal calf serum. For stable expression of MSP, cells in 10-cm dishes were transfected with 10 μg of MSP cDNA by Superfect reagent (Qiagen, Santa Clarita, CA) and placed in medium with 500 μg/ml geneticin (Life Technologies, Inc.). After selection, single colonies were cloned, and clones with highest equal expression of wild type and mutant MSP were selected. The concentration of recombinant MSP in culture supernatants was measured by sandwich ELISA.

Sandwich ELISA for MSP—The concentration of secreted recombinant MSP in cell culture supernatants was determined by sandwich ELISA (28). Concentrations were calculated by reference to a standard curve generated with wild type recombinant human MSP.

Immunoprecipitation and Western Blotting—MSP from culture supernatants was immunoprecipitated by rabbit polyclonal anti-MSP antibodies conjugated to Sepharose beads. Immunoprecipitates were washed and boiled after addition of 2× sample buffer. After PAGE, proteins were transferred to a nitrocellulose membrane (Amersham Pharmacia Biotech). MSP was detected with rabbit anti-MSP antibodies. ECL (Amersham Pharmacia Biotech) was used for visualization of the peroxidase complex.

Metabolic Labeling of MSP—CHO-K1 cells stably expressing wild type or mutant MSP were incubated for 48 h with ^{35}S-easy labeling mix ([^{35}S]cysteine and [^{35}S]methionine) (NEN Life Science Products) in methionine- and cysteine-free Dulbecco's modified Eagle's medium (Life Technologies, Inc.) supplemented with 8% dialyzed fetal calf serum. The quality and quantity of ^{35}S-labeled MSP were analyzed by immunoprecipitation and SDS-PAGE under reducing and non-reducing conditions.

Binding and Competition Assays with ^{35}S-Labeled MSP—MDCK-RE7 cells with stably expressed RON receptor were used. The parental MDCK cell line without detectable expression of RON was used as a negative control. Five ml of supernatant containing equal concentrations of ^{35}S-labeled wild type or mutant MSP were added to 5×10^6 RE7 or MDCK cells. Cells were equilibrated for 4 h at 4 °C. After equilibration, cells were washed 3 times with phosphate-buffered saline and lysed in lysis buffer (50 mM HEPES, pH 7.4, 150 mM NaCl, 10% glycerol, 1 mM EDTA, 1 mM sodium orthovanadate, 10 mM sodium pyrophosphate, 100 mM NaF, 1% Triton X-100, 10 μg/ml leupeptin, 10 units/ml aprotinin, 1 mM phenylmethylsulfonyl fluoride). After clarification, lysates were immunoprecipitated by equilibration overnight at 4 °C with rabbit anti-MSP antibodies coupled to Sepharose. Then immunoprecipitates were washed 3 times with HNTG buffer (50 mM HEPES, pH 7.4, 150 mM NaCl, 10% glycerol, 0.1% Triton X-100) and analyzed by SDS-PAGE. Protein bands were detected by radioautography. For competition assays, 50 nM unlabeled recombinant human MSP or free α or β chains were equilibrated with cells together with ^{35}S-labeled MSP culture supernatants.

Binding of Free α Chain to RON Receptor—RE7 cells (5×10^6/well) with stably expressed RON receptor and parental MDCK cells as a negative control were equilibrated for 4 h at 4 °C in 5 nM free recombinant α chain or MSP. Cells were then washed, and cell lysates were processed as described above, except that detection of protein bands was by immunoblotting with polyclonal rabbit anti-MSP antibodies.

RON-ELISA—ELISA microtiter plates were coated overnight at 4 °C with the recombinant mouse MSP receptor RON/Fc (rmRON/Fc) chimera (R & D Systems, Inc.) (100 μl/well at 0.5 μg/ml in carbonate-bicarbonate buffer, pH 9.6). Nonspecific binding sites were blocked with 1% bovine serum albumin for 1 h at 37 °C. RON-coated ELISA plates were then incubated for 2 h with a series of 2-fold dilutions of human recombinant MSP (highest concentration 6.4 nM), free β chain (highest concentration 8 nM) or free α chain (highest concentration 320 nM). ELISA plates were washed 3 times with TBS/Tween 20 after this and subsequent steps. Plates were then incubated with rabbit polyclonal anti-MSP for an additional 2 h. The rabbit anti-MSP antibodies recognize MSP and separate free chains with comparable sensitivity, as determined by direct ELISA in which microtiter wells were coated with MSP or free α or β chain standards (data not shown). Bound rabbit anti-MSP was detected by equilibration with alkaline phosphatase-conjugated anti-rabbit IgG. Substrate 104 (Sigma) was used for quantifying alkaline phosphatase activity. Absorbance at 405 nM was measured with an ELISA reader. At least three independent experiments were performed. To quantify ligand binding affinity, EC_{50} values were calculated by using a four-parameter nonlinear fitting algorithm (31).

RESULTS

Model of the Serine Protease Domain of MSP—The structural core of all chymotrypsin-like serine proteases is composed of two six-stranded β barrels, with the active site in a crevice between these two domains. MSP and HGF β chains have 48% sequence identity (Fig. 1) and higher than 30% sequence similarity to several mammalian serine proteases. Features in common include the same bilobed core, several surface loops, and a C-terminal helix (Fig. 2*A*). Furthermore, despite loss of enzymatic activity because of catalytic triad mutations, the geometry of the regions of MSP that correspond to the active site of serine proteases has been conserved. This includes mutated catalytic triad residues Gln^{522}(57),[3] Gln^{568}(102), and Tyr^{661}(195) (colored *magenta* in Figs. 1 and 2) at the junction of the β barrels, the same conformation of the Gly^{655}(189)-Asp^{660}(194) segment (colored *violet*) necessary for the formation of an oxyanion hole and a mature substrate specificity pocket. The critical interaction maintaining active site architecture, a salt bridge between Asp^{660}(194) and the NH_3^+ group from the N-terminal Val of the β chain, is conserved.

The residues critical for zymogen activation (for a review see Ref. 32) are also conserved in MSP, suggesting that conversion to the biologically active growth factor conformation mirrors the mechanism of zymogen activation. In the zymogen form of the chymotrypsin-like enzymes, the active site cleft is not completely formed. His^{505}(40) interacts with Asp^{660}(194), and the adjacent segment Gly^{655}(189)-Asp^{660}(194) is oriented to the

[3] MSP residue numbers in the text are followed in parentheses by the corresponding bovine trypsin residue number.

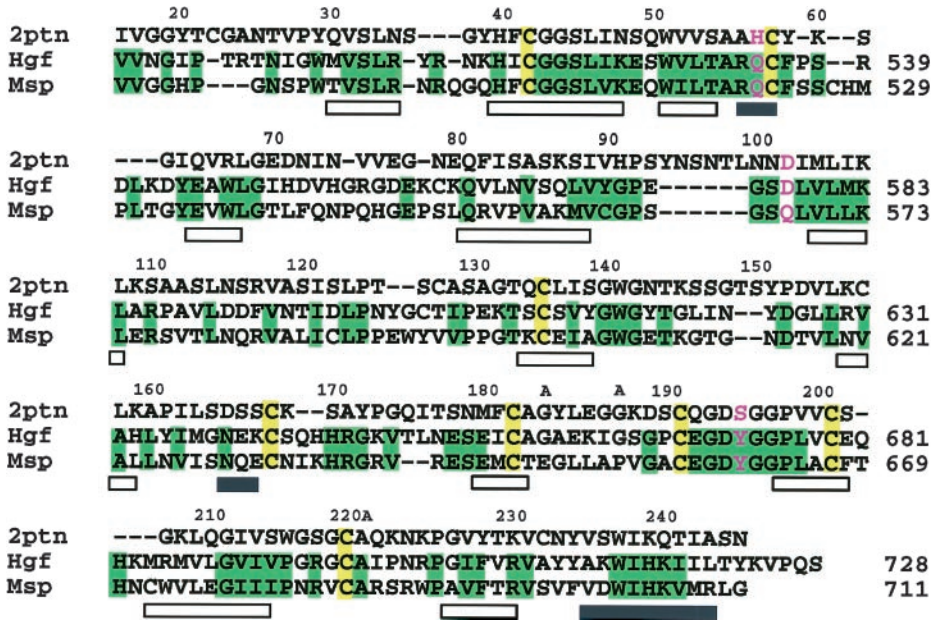

FIG. 1. **Sequence alignment of bovine trypsin and serine protease domains of HGF and MSP.** Conserved cysteines are marked in *yellow*; sequence homology between HGF and MSP is shown in *green*. Residues corresponding to the catalytic triad are shown in *magenta*. *Numbering* at the *top* corresponds to that of 2PTN entry in the Protein Data Bank. The *open* and *filled bars* under the sequence show the locations of β strands and helices, respectively.

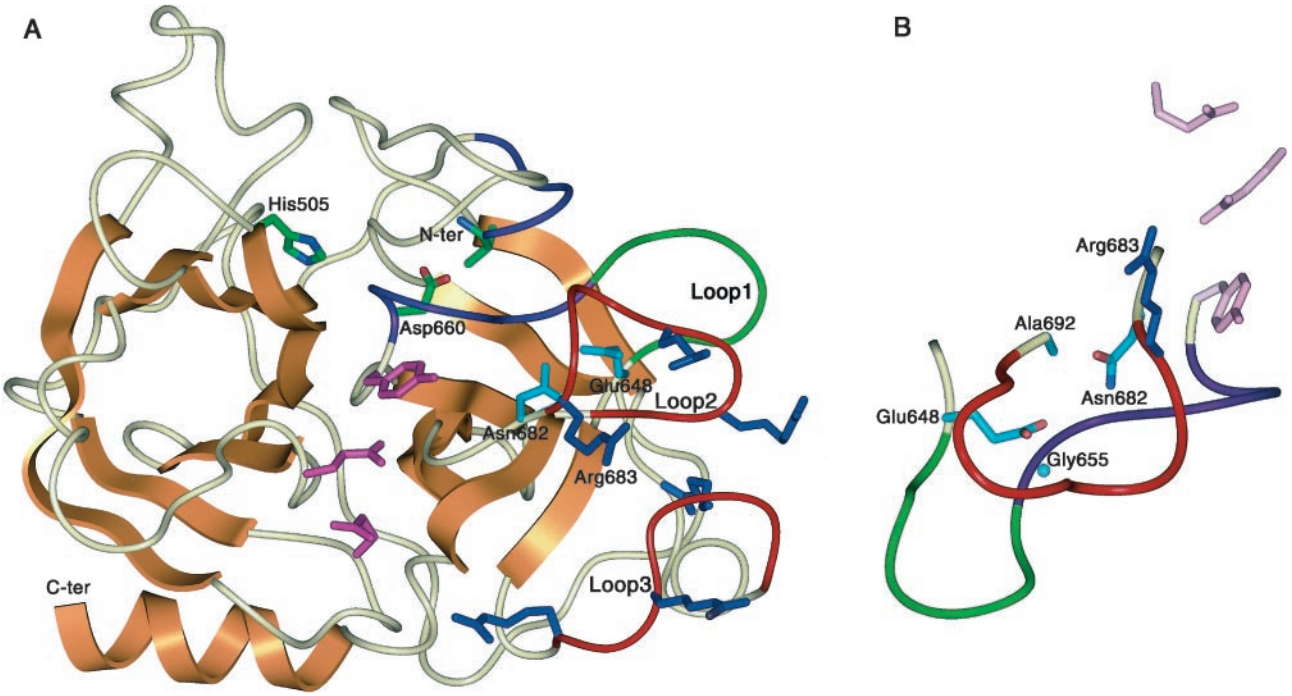

FIG. 2. **A ribbon representation of the three-dimensional model of MSP serine protease domain.** β-Strands and C-terminal α helix are shown in *orange*. Surface loop 1 (*colored green*) contains exclusively hydrophobic amino acids Leu, Leu, Ala, Pro, and Val. Three Arg residues from loop 2 (*red*) and three from loop 3 (*red*) form a prominent cluster of positive charge on the MSP surface. Segments with conformation significantly different from that of chymotrypsinogen, 484(16)-489(21) and 645(189)-660(194) are colored *violet*. Side chains of several key amino acids are also shown: mutated catalytic triad, Gln^{522}(57), Gln^{568}(102), Tyr^{661}(195) in *magenta*; Glu^{648}(184) and Asn^{682}(216) buried in the S1 substrate binding pocket in *azure*; cluster of Arg residues in *dark blue*; carbon atoms of residues critical for zymogen activation, Val^{484}(16), Asp^{660}(194), and His^{505}(40) in *green*. *B,* close-up of the region corresponding to the S1 specificity pocket of trypsin with the side chains of critical residues. Coloring as in *A*.

interior of the zymogen. Upon activation, Asp^{660}(194) forms the salt bridge noted above with the newly liberated N terminus, and segment Gly^{655}(189)-Asp^{660}(194) (colored *violet* in Fig. 2*A*) moves outward toward solvent to complete the active site cleft.

Surface loop features specific for MSP are noted in the legend of Fig. 2*A*. A detailed view of the region of MSP corresponding to the substrate binding pocket and catalytic triad is shown in Fig. 2*B*. Several features distinguish MSP from trypsin in this region as follows: 1) The entrance to the large cylindrical S1 pocket is blocked in MSP by Asn^{682}(216) and Ala^{692}(226), in contrast to trypsin, which has Gly residues at these positions. The conformation of Asn^{682}(216) is stabilized by interaction with Glu^{648}(184) buried inside the pocket. 2) Residue 655 in the base of the pocket in MSP is Gly, whereas in trypsin it is Asp, which interacts with the scissile bond Lys of the substrate. Thus, the model suggests that the receptor binding region of MSP does not include the base of the S1 pocket but involves the entrance.

Characterization of MSP Produced by CHO Cells Stably Transfected with Wild Type and Mutated MSP cDNAs—Two MSP mutants were generated, a double mutant of residues that stabilize the shape of the S1 pocket (E648G/N682G) and a mutation of Arg^{683} (R683Q), adjacent to the entrance to the S1 pocket. Wild type and mutated MSP cDNAs were cloned into

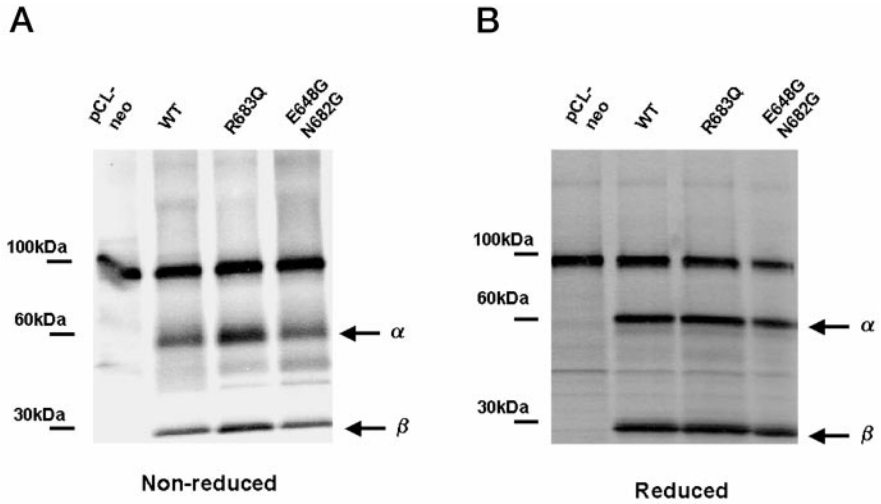

FIG. 3. **Analysis by SDS-PAGE under non-reduced (*A*) and reduced (*B*) conditions of ^{35}S-labeled MSP produced by CHO cells.** CHO cells with stably expressed wild type (*WT*) or mutated MSP were metabolically labeled with [^{35}S]methionine and -cysteine. ^{35}S-Labeled MSP was immunoprecipitated from 1 ml of CHO tissue culture supernatants by rabbit anti-MSP antibodies coupled to Sepharose beads. Immunoprecipitated proteins were separated by 4–12% gradient SDS-PAGE under non-reducing (*A*) and reducing (*B*) conditions and detected by radioautography. *Arrows* indicate the position of MSP α and β chains. Their presence under non-reducing conditions shows that they are not disulfide-linked. The band at about 90 kDa is not an MSP protein.

the eukaryotic expression vector pCl-neo, and stable CHO cell transfectants were generated. Serum-containing medium from the transfected cells was used as a source of wild type and mutant MSP. We selected clones that produced equal amounts of wild type or mutant MSP, and by sandwich ELISA the concentration in the medium was 0.5 nM (data not shown). The products were further characterized by SDS-PAGE. Culture fluids from ^{35}S-metabolically labeled CHO cell transfectants were immunoprecipitated by rabbit anti-MSP antibodies and analyzed by SDS-PAGE under non-reducing and reducing conditions (Fig. 3). In confirmation of the sandwich ELISA results, the intensity of the bands in Fig. 3 shows that the selected CHO cell clones produce comparable amounts of wild type or mutated MSP. SDS-PAGE under reducing conditions shows that there is no 80-kDa pro-MSP in CHO supernatants. Only two bands at molecular mass positions of approximately 60 and 30 kDa corresponding to MSP α and β chains were visualized (Fig. 3*B*). This is due to the fact that recombinant pro-MSP is cleaved to MSP in supernatants of CHO cells cultured in medium containing serum (17). The absence of an 80-kDa band under non-reducing conditions (Fig. 3*A*) demonstrates that the α and β chains of these recombinant products are not disulfide-linked, in contrast to αβ chain heterodimeric native MSP. This is due to the fact that in recombinant pro-MSP, β chain Cys^{588} may form an intrachain disulfide with Cys^{672} instead of with α chain Cys^{468} (19, 33).

Binding of Wild Type and Mutated MSP β Chain to RON—To determine the capacity of wild type and mutated MSP β chain to interact with receptor, MDCK-RE7 cells with overexpressed RON and parental MDCK cells as a control were equilibrated with ^{35}S-labeled CHO cell supernatants containing 0.5 nM free α and β chain. After equilibration, cells were washed and lysed. Cell-bound MSP chains were immunoprecipitated by rabbit anti-MSP antibodies which recognize both α and β chains (28). Precipitated MSP chains were analyzed by SDS-PAGE, and protein bands were visualized by radioautography. Results for RE7 lysates (Fig. 4*A*) showed an intense wild type MSP β chain band, a faint band for β chain mutated in the S1 pocket, and no band for the R683Q mutant. Densitometry of the β chain bands showed that the amount of double mutant E648G/N682G bound was about 50 times less than bound wild type β chain; no R683Q band was detected. There was no MSP

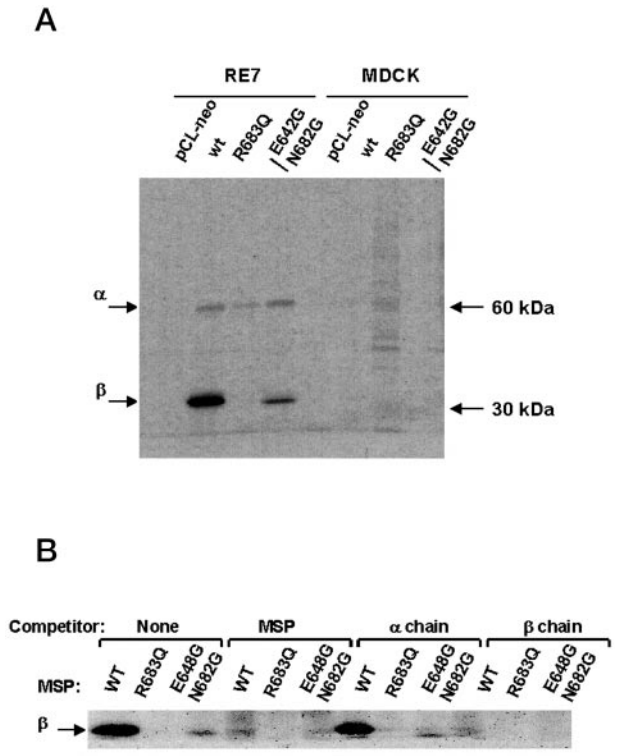

FIG. 4. *A,* binding of ^{35}S-labeled wild type (*WT*) and mutated MSP to RON. MDCK-RE7 cells (5×10^6) with stably expressed RON receptor or parental MDCK cells without detectable RON were equilibrated for 4 h at 4 °C in 5 ml of CHO tissue culture supernatants containing ^{35}S-labeled wild type or mutated MSP. Cell-bound ^{35}S-MSP was immunoprecipitated with rabbit anti-MSP antibodies coupled to Sepharose beads. Immunoprecipitated proteins were separated by 4–12% gradient SDS-PAGE, and protein bands were visualized by radioautography. *B*, MSP and free β chain compete with ^{35}S-labeled wild type or mutated MSP for binding to RON. MDCK-RE7 cells were equilibrated for 4 h at 4 °C in 5 ml of CHO supernatants containing ^{35}S-labeled wild type or mutated MSP in the presence of excess unlabeled MSP, α chain or β chain. Cell-bound labeled MSP was detected as described for *A*.

β chain binding to parental MDCK cells, which do not express detectable RON (9). Interaction of ^{35}S-labeled β chain from CHO supernatants was inhibited by either unlabeled MSP or

free β chain (Fig. 4*B*). This result suggested that we were observing saturable binding of β chain to RON, a conclusion supported by the absence of binding to MDCK cells. The diminished or absent β chain mutant bands in Fig. 4*A* therefore reflect diminished or undetectable binding of the mutants to RON.

Binding of Free α Chain to MDCK-RE7 Cells—In addition to the β chain, we detected binding of free α chain to RON-expressing cells (Fig. 4*A, upper band*). Reasons to suggest that the observed band represents MSP α chain are as follows: 1) an appropriate molecular mass; 2) no band in the case of supernatants from metabolically labeled CHO cells transfected with vector alone, which therefore do not express MSP; and 3) no band with supernatants of MSP-transfected cells that were equilibrated with parental MDCK cells, which do not express RON. Comparison of the band intensities in Fig. 4*A* shows that the amount of bound α chain is only a small fraction of the amount of bound β chain. Therefore it was important to determine whether the band reflected binding of free α chain or a small amount of MSP $\alpha\beta$ chain heterodimer binding via the β chain. Two facts weighed against the latter possibility. First, as noted above, SDS-PAGE of metabolically labeled transfected CHO cell supernatants did not reveal any trace of $\alpha\beta$ chain MSP. Second, despite no sign of MSP mutant R683Q β chain binding, the α chain band was detectable (Fig. 4*A*). To obtain independent evidence that free α chain can interact with RON, a binding assay of purified recombinant α chain was performed. MDCK-RE7 cells or MDCK cells as a control were equilibrated for 4 h at 4 °C with 5 nM free recombinant α chain or disulfide-linked $\alpha\beta$ chain MSP. Then bound $\alpha\beta$ chain MSP or α chain was immunoprecipitated with mouse monoclonal 2 S anti-MSP, which recognizes only α chain (28). Immunoprecipitated α chain was detected on a blot with rabbit anti-MSP antibodies after SDS-PAGE and transfer of proteins to a nitrocellulose membrane. Fig. 5*A* shows binding of free α chain to RE-7 cells, which is a small fraction of the amount of α chain detected after $\alpha\beta$ chain MSP was equilibrated with the cells. In both cases, binding is RON-dependent, as shown by the absence of bands from MDCK cell lysates. It was also important to consider the possibility that the bound α chain line came from binding of a small amount of $\alpha\beta$ MSP that contaminates the α chain preparation. This was ruled out by SDS-PAGE of the same cell immunoprecipitates under non-reducing conditions. If the α chain detected in Fig. 5*A* (under reducing conditions) were due entirely to bound $\alpha\beta$ chain contaminating the α chain preparation, non-reducing SDS-PAGE should show an $\alpha\beta$ line and no α. The converse is the case (Fig. 5*B*). For the α chain lane, at an ECL exposure that shows an α chain line comparable in intensity to that of Fig. 5*A*, there is no detectable $\alpha\beta$ line. At longer exposure times we see an $\alpha\beta$ line and a much more intense α chain line. The latter reflects binding of free α chain to the RE-7 cells; the former is due to the small amount of $\alpha\beta$ chain contaminating the α chain preparation and is a small fraction of the total bound α chain.

Quantitative Analysis of MSP, α and β Chain Binding to the RON Receptor—In addition to the above experiments on binding of MSP and its chains to cells expressing RON, we quantified by sandwich ELISA the binding of disulfide-linked $\alpha\beta$ chain MSP and free α and β chains to recombinant mouse RON receptor adsorbed to wells of a microtiter plate. Binding of each ligand was tested in duplicate in three separate experiments, and concentration-dependent binding curves were generated (Fig. 6). Mean EC_{50} values calculated from curves of the three experiments (31) are shown in the *inset* of Fig. 6. Disulfide-linked $\alpha\beta$ chain MSP has a somewhat higher affinity for RON than free β chain, a result comparable to binding data for

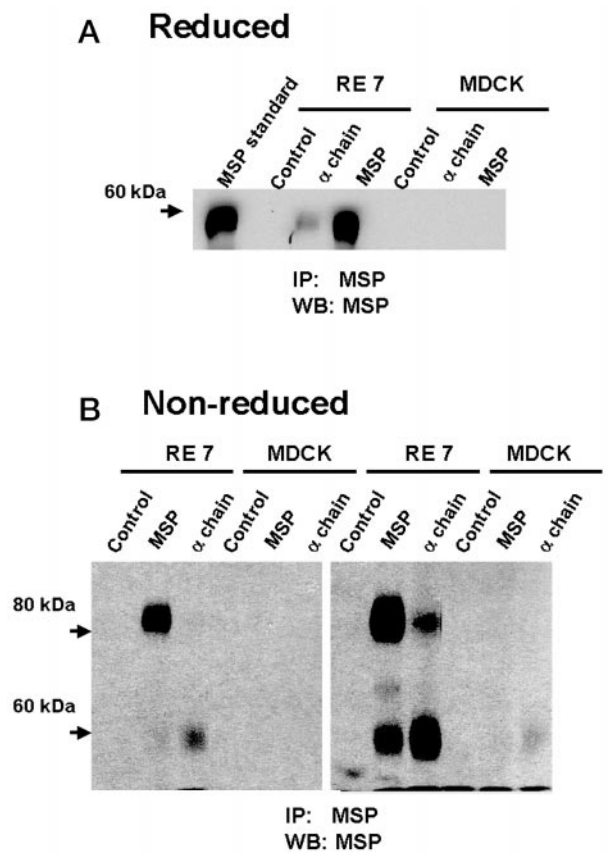

FIG. 5. **Interaction of MSP free α chain with RON.** MDCK-RE7 cells or MDCK cells as a control were equilibrated for 4 h at 4 °C in 5 nM recombinant MSP or free α chain. Cell-bound MSP or α chain was immunoprecipitated (*IP*) by mouse monoclonal anti-MSP antibody (that reacts with an α chain epitope) coupled to Sepharose. Immunoprecipitated proteins were separated by 7.5% SDS-PAGE under reducing (*A*) and non-reducing (*B*) conditions. Protein bands were detected by Western blotting (*WB*) with rabbit anti-MSP antibodies. For the MSP standard, 5 nM MSP was directly immunoprecipitated with mouse monoclonal anti-MSP. The *left* and *right* blots in *B* illustrate results of short and long exposures.

RON-expressing cells (24). In contrast, free α chain binds to RON with a much lower affinity, as reflected in an EC_{50} that is 2 orders of magnitude higher than the value for MSP. Thus, MSP has two separate binding sites with high and low affinity, located in β and α chains, respectively.

DISCUSSION

The MSP β chain three-dimensional model enabled us to consider possible loci for RON high affinity binding by analogy to substrate-enzyme interactions in the family of chymotrypsin-like serine proteases. In zymogens of the family the catalytic triad is formed, but the substrate-binding site is not fully shaped. MSP is able to bind RON with high affinity only after proteolytic cleavage, which in zymogens causes conformational changes leading to formation of a mature binding site (Fig. 2). Thus residues critical for receptor binding should correspond to those that define the subsite preference at the scissile bond of substrate. According to the model, the S1 pocket in MSP is filled by interacting pair Glu^{648} and Asn^{682}, leaving only a shallow cavity for interaction with the substrate side chain. In addition to a double mutant of the Glu/Asn pair (E648G/N682G), we made a single mutant of Arg^{683} located at the entrance to the S1 pocket. We mutated Arg^{683} to Gln, which is also hydrophilic and has side chain length comparable to that of Arg. Thus mutation of Arg^{683} to Gln was not expected to affect the structure of the β chain. The fact that mutation of

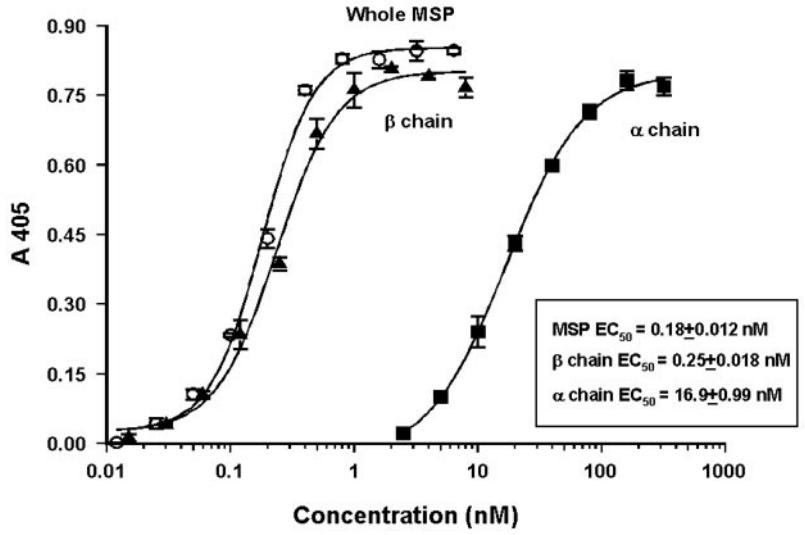

FIG. 6. **Concentration-dependent binding of recombinant disulfide-linked αβ chain MSP and free α and β chains to the RON receptor adsorbed to wells of a microtiter plate and measured in an ELISA as described under "Experimental Procedures."** Each value represents the mean ± S.E. of three independent experiments.

Arg^{683} alone completely abolished β chain binding to RON (Fig. 4*A*) suggests that this residue is directly involved in receptor binding. Such a profound effect caused by a single site mutation is not surprising in view of the fact that mutation of a single residue of human growth hormone receptor (34) or HGF α chain (see below) caused loss of binding to their respective ligands. Binding of β chain mutant E648G/N682G is about 50 times less than the binding of β chain wild type. The diminished binding of the double mutant (E648G/N682G) suggests that these residues are required to stabilize the β chain structure in this region. Our results show that the region corresponding to an enzyme S1 site is essential for β chain binding to RON. Other features affecting specificity of MSP-receptor interactions may involve residues from loops 1–3 (shown in Fig. 2*A*), which influence substrate specificity and catalytic efficiency of the trypsin-like serine proteases (26). It is noteworthy that six Arg side chains from loops 2 and 3 form a prominent cluster of positive charge on the MSP β chain surface in the neighborhood of the S1 site.

We recently proposed that both HGF and MSP have two receptor binding sites of different affinity, one on the α chain and one on the β chain, and that Met and RON dimerization can be induced by a single ligand molecule (27). The site on the β chain becomes available for binding only after proteolytic cleavage of the single chain precursors. For HGF, the high affinity site is on the α chain and the postulated low affinity site is on the β chain. The converse is the case for MSP. Comparison of our model of the MSP β chain structure with that of the HGF β chain shows that, in contrast to MSP, the opening of the HGF S1 pocket is not blocked; and there are differences in the surface loops, as described in the legend of Fig. 2*A*. These differences in the S1 pocket and neighboring surface loops could account for the inability of HGF to bind via its β chain to RON (35).

This communication provides the first evidence that free MSP α chain interacts with the RON receptor (Figs. 4*A*, 5, and 6). We previously reported undetectable binding to RON-expressing cells by a ^{125}I-labeled aliquot of the same α chain preparation used in the current study (24). We attribute this to a lower sensitivity of the former method. After cells were equilibrated with equimolar concentrations of free α and β chains, bound α chain was less than 10% of bound β chain (determined by densitometry of the blot shown in Fig. 4*A*). The published binding curves of iodinated MSP or β chain show that 10% of the observed values would be indistinguishable from background (24). We quantified binding of MSP and its free α and β chains to recombinant RON adsorbed to microtiter wells. Results show that MSP has two binding sites with low (EC_{50} = 16.9 nM) and high (EC_{50} = 0.25 nM) affinity, located in α and β chains respectively.

Despite binding of free α chain or β chain to RON, neither chain can replicate the action of the disulfide-linked heterodimer. Wang *et al.* (24) reported that whereas mature MSP caused tyrosine phosphorylation of RON and a cellular biological response, these effects were not induced by strongly binding free β chain or by α chain. In our case, the low level of α chain binding to RON-expressing cells also did not induce RON tyrosine phosphorylation (data not shown). How does αβ chain MSP cause RON dimerization? The fact that the α chain and β chain are each capable of interacting with RON suggests that MSP is bivalent, with a high affinity locus on the β chain and a low affinity site on the α chain. The contribution of the α chain to the binding strength of MSP to RON was suggested by an MSP binding K_d that was significantly lower than the K_d for free β chain (24). As noted above, we proposed that a RON dimer could be formed by a single MSP molecule that could bind to RON via the β chain, after which a second RON could interact with the α chain. The converse sequence was suggested for HGF. This is the model that has been confirmed for induction of receptor dimerization by growth hormone (36). The finding that the α chain can bind to RON supports our proposed model.

Acknowledgments—We thank Dr. Tom L. Blundell and colleagues for providing us with the coordinates of the HGF β chain three-dimensional model. We also thank Dr. Teizo Yoshimura for the MSP cDNA and Alison Skeel for technical assistance.

REFERENCES

1. Skeel, A., Yoshimura, T., Showalter, S., Tanaka, S., Appella, E., and Leonard, E. (1991) *J. Exp. Med.* **173,** 1227–1234
2. Yoshimura, T., Yuhki, N., Wang, M.-H., Skeel, A., and Leonard, E. J. (1993) *J. Biol. Chem.* **268,** 15461–15468
3. Han, S., Stuart, L. A., and Degen, S. J. F. (1991) *Biochemistry* **30,** 9768–9780
4. Leonard, E. J. (1997) in *Plasminogen-related Growth Factors* (Bock, G. R., and Goode, J. A., eds) pp. 183–191, John Wiley & Sons, Inc., New York
5. Leonard, E. J., and Skeel, A. (1976) *Exp. Cell Res.* **102,** 434–438
6. Wang, M.-H., Cox, G. W., Yoshimura, T., Sheffler, L. A., Skeel, A., and Leonard, E. J. (1994) *J. Biol. Chem.* **269,** 14027–14031
7. Danilkovitch, A., and Leonard, E. J. (1999) *J. Leukocyte Biol.* **65,** 345–348
8. Ronsin, C., Muscatelli, F., Mattei, M. G., and Breathnach, R. (1993) *Oncogene* **8,** 1195–1202
9. Wang, M.-H., Ronsin, C., Gesnel, M.-C., Coupey, L., Skeel, A., Leonard, E. J., and Breathnach, R. (1994) *Science* **266,** 117–119
10. Wang, M.-H., Iwama, A., Skeel, A., Suda, T., and Leonard, E. J. (1995) *Proc. Natl. Acad. Sci. U. S. A.* **92,** 3933–3937
11. Iwama, A., Wang, M.-H., Yamaguchi, N., Okano, K., Sudo, T., Gervais, F., Morissette, C., Leonard, E. J., and Suda, T. (1995) *Blood* **86,** 3394–3403
12. Matsumoto, K., and Nakamura, T. (1992) *Crit. Rev. Oncog.* **3,** 27–54

13. Park, M., Dean, M., Kaul, K., Braun, M. J., Gonda, M. A., and Vande Woude, G. (1987) *Proc. Natl. Acad. Sci. U. S. A.* **84,** 6379–6383
14. Matsumoto, K., and Nakamura, T. (1997) *Biochem. Biophys. Res. Commun.* **239,** 639–644
15. Jeffers, M., Rong, S., and Woude, G. F. (1996) *J. Mol. Med.* **74,** 505–513
16. Schmidt, L., Duh, F. M., Chen, F., Kishida, T., Glenn, G., Choyke, P., Scherer, S. W., Zhuang, Z., Lubensky, I., Dean, M., Allikmets, R., Chidambaram, A., Bergerheim, U. R., Feltis, J. T., Casadevall, C., Zamarron, A., Bernues, M., Richard, S., Lips, C. J., Walther, M. M., Tsui, L. C., Geil, L., Orcutt, M. L., Stackhouse, T., and Zbar, B. (1997) *Nat. Genet.* **16,** 68–73
17. Wang, M.-H., Yoshimura, T., Skeel, A., and Leonard, E. J. (1994) *J. Biol. Chem.* **269,** 3436–3440
18. Bezerra, J. A., Witte, D. P., Aronow, B. J., and Degen, S. J. (1993) *Hepatology* **18,** 394–399
19. Yoshikawa, W., Hara, H., Takehara, T., Shimonishi, M., Sakai, H., Shimizu, N., Shimizu, S., Wang, M.-H., Hagiya, M., Skeel, A., and Leonard, E. J. (1999) *Arch. Biochem. Biophys.* **363,** 356–360
20. Nanney, L. B., Skeel, A., Luan, J., Polis, S., Richmond, A., Wang, M.-H., and Leonard, E. J. (1998) *J. Invest. Dermatol.* **111,** 573–581
21. Donate, L. E., Gherardi, E., Srinivasan, N., Sowdhamini, R., Aparicio, S., and Blundell, T. L. (1994) *Protein Sci.* **3,** 2378–2394
22. Sakata, H., Stahl, S. J., Taylor, W. G., Rosenberg, J. M., Sakaguchi, K., Wingfield, P. T., and Rubin, J. S. (1997) *J. Biol. Chem.* **272,** 9457–9463
23. Lokker, N. A., Presta, L. G., and Godowski, P. J. (1994) *Protein Eng.* **7,** 895–903
24. Wang, M. H., Julian, F. M., Breathnach, R., Godowski, P. J., Takehara, T., Yoshikawa, W., Hagiya, M., and Leonard, E. J. (1997) *J. Biol. Chem.* **272,** 16999–17004
25. Waltz, S. E., McDowell, S. A., Muraoka, R. S., Air, E. L., Flick, L. M., Chen, Y. Q., Wang, M. H., and Degen, S. J. (1997) *J. Biol. Chem.* **272,** 30526–30537
26. Perona, J. J., and Craik, C. S. (1997) *J. Biol. Chem.* **272,** 29987–29990
27. Miller, M., and Leonard, E. J. (1998) *FEBS Lett.* **429,** 1–3
28. Wang, M.-H., Skeel, A., Yoshimura, T., Copeland, T. D., Sakaguchi, K., and Leonard, E. J. (1993) *J. Leukocyte Biol.* **54,** 289–295
29. Jones, A. (1985) *Methods Enzymol.* **115,** 157–171
30. Brunger, A. (1992) *X-PLOR: A System for X-ray Crystallography and NMR*, version 3.1, Yale University Press, New Haven, CT
31. Jin, L., Fendly, B. M., and Wells, J. A. (1992) *J Mol. Biol.* **226,** 851–865
32. Khan, A. R., and James, M. N. (1998) *Protein Sci.* **7,** 815–836
33. Wahl, R. C., Costigan, V. J., Batac, J. P., Chen, K., Cam, L., Courchesne, P. L., Patterson, S. D., Zhang, K., and Pacifici, R. E. (1997) *J. Biol. Chem.* **272,** 15053–15056
34. Clackson, T., and Wells, J. A. (1995) *Science* **267,** 383–386
35. Wang, M.-H., Iwama, A., Dlugosz, A. A., Sun, Y., Skeel, A., Yuspa, S. H., Suda, T., and Leonard, E. J. (1996) *Exp. Cell Res.* **226,** 39–46
36. de Vos, A. M., Ultsch, M., and Kossiakoff, A. A. (1992) *Science* **255,** 306–312